



SHORT COMMUNICATION

Metabolic acclimation to hypoxia revealed by metabolite gradients in melon fruit

Benoît Biais^{a,c,*}, Bertrand Beauvoit^{a,b,c}, J. William Allwood^d, Catherine Deborde^{a,c}, Mickaël Maucourt^{a,b,c}, Royston Goodacre^d, Dominique Rolin^{a,b,c}, Annick Moing^{a,c}

^a INRA, UMR619 Fruit Biology, Centre INRA de Bordeaux, 71 Ave Edouard Bourlaux, F-33140 Villenave d'Ornon, FR, France

^b Université de Bordeaux, UMR619 Fruit Biology, Centre INRA de Bordeaux, 71 Ave Edouard Bourlaux, F-33140 Villenave d'Ornon, FR, France

^c Plateforme Métabolome-Fluxome – Centre de Génomique Fonctionnelle de Bordeaux, IFR103 BVI, Centre INRA de Bordeaux, 71 Ave Edouard Bourlaux, F-33140 Villenave d'Ornon, FR, France

^d School of Chemistry, Manchester Interdisciplinary Biocentre, The University of Manchester, 131 Princess Street, Manchester M1 7DN, UK

ARTICLE INFO

Article history:

Received 6 May 2009

Received in revised form

14 August 2009

Accepted 17 August 2009

Keywords:

Cucumis melo

Hypoxia

Melon fruit

Metabolite gradients

Metabolic profiling

ABSTRACT

A metabolomics approach using ¹H NMR and GC–MS profiling of primary metabolites and quantification of adenine nucleotides with luciferin bioluminescence was employed to investigate the spatial changes of metabolism in melon fruit. Direct ¹H NMR profiling of juice collected from different locations in the fruit flesh revealed several gradients of metabolites, e.g. sucrose, alanine, valine, GABA or ethanol, with increase in concentrations from the periphery to the center of the fruit. GC–MS profiling of ground samples revealed gradients for metabolites not detected using ¹H NMR, including pyruvic and fumaric acids. The quantification of adenine nucleotides highlighted a strong decrease in both ATP and ADP ratios and the adenylate energy charge from the periphery to the center of the fruit. These concentration patterns are consistent with an increase in ethanol fermentation due to oxygen limitation and were confirmed by observed changes in alanine and GABA concentrations, as well as other markers of hypoxia in plants. Ethanol content in melon fruit can affect organoleptic properties and consumer acceptance. Understanding how and when fermentation occurred can help to manage the culture and limit ethanol production.

© 2009 Elsevier GmbH. All rights reserved.

Introduction

Melon (*Cucumis melo*), one of the oldest cultivated crops, is widely cultivated across the world. According to the FAO, world production of melons in 2007 was about 26 million tons (<http://www.fao.org>). The numerous species differ greatly in fruit size (from a few grams to several kilograms), morphology (round to elongated shape) and organoleptic properties (bitter to sweet) (Stepansky et al., 1999). The French melon sp. Charentais is extensively consumed in Europe during the summer, as its orange flesh is freshening and sweet with a pleasant aroma. Melon fruit is also a healthy human food, providing nutrients and antioxidants such as β-carotene and vitamins (C, E and folic acid) (de Melo et al., 2000).

Abbreviations: ¹H NMR, proton nuclear magnetic resonance; AEC, adenylate energy charge; GABA, gamma amino butyric acid; GC–MS, gas chromatography–mass spectrometry; PDC, pyruvate decarboxylase; TCA, tri carboxylic acids

* Corresponding author at: INRA, UMR619 Fruit Biology, Centre INRA de Bordeaux, 71 Ave Edouard Bourlaux, F-33140 Villenave d'Ornon, FR, France. Tel.: +33 557 122 695; fax: +33 557 122 541.

E-mail addresses: benoit.biais@bordeaux.inra.fr, bbiais@free.fr (B. Biais).

The most important properties of melon for fruit organoleptic quality and consumer's acceptance are the aroma profile (Kourkouts et al., 2006) and the sucrose level (Stepansky et al., 1999b). Several aspects of sugar metabolism have therefore been studied, including the transport of stachyose and raffinose within the phloem and their translocation into the fruit (Lalonde et al., 2003), and sucrose accumulation during fruit development and ripening (Burger and Schaffer, 2007).

Few data relating to the spatial changes of metabolite concentrations in melon fruit flesh are available. However, near infra-red imaging has been used to analyze the sugar localization in melon slices (Sugiyama, 1999). Recently, a metabolomic approach using ¹H NMR and GC–EI–TOF–MS profiling was used to assess both the concentration and spatial localization of the main primary metabolites in various cultivars of melon fruit (Biais et al., 2009). Part of the latter study suggested the existence of several metabolite gradients within the fruit. These may be related to *in situ* hypoxia in the central part of the ripening fruit; similar results were obtained on pear fruit under low oxygen stress (Pedreschi et al., 2009). To verify this hypothesis, in parallel with quantification of primary metabolites, adenine nucleotides were quantified in melon fruit, allowing the comparison of the metabolite composition with the energy status of the tissue.

Materials and methods

Plant material

The seeds of F1 hybrid melon (*Cucumis melo* cv. Cézanne) were obtained from Clause-Tézier (France). Plants were grown in an open field in south-western France (Moissac, 44°06'17"N × 1°04'41"E) between April and July, 2007. The soil type was clay and limestone and the plant density was 9200 plants/ha. Irrigation, watering, fertilization and pathogen-pest control were performed according to standard commercial practices. Fruits were harvested at 3/4 slip maturity. Analyses were performed within 4 h after harvest.

Sampling and analyses of melon flesh pieces

One representative melon fruit was cut in half lengthwise and three slices were cut; two for metabolite analyses (¹H NMR and GC–MS) and the other for adenine nucleotide analyses (thickness: 1 cm). The slices were divided into five small sections (7 mm × 7 mm), cut from the skin position 1, epicarp+green mesocarp) to the

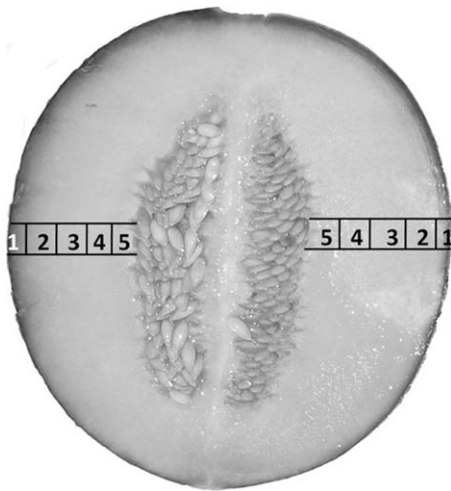


Fig. 1. Representation of the location of collected flesh pieces for ¹H NMR and GC–MS profiling and adenine nucleotide quantification in melon slices. Position 1 corresponds to the epicarp+green mesocarp, and positions 2–5 to the orange mesocarp.

center of the fruit (position 5, inner orange mesocarp) according to Fig. 1, in two different areas on the equatorial plane of the slice. The refractive index (Brix %) of fresh juice was measured immediately after sampling and increased regularly from 6.3% ± 0.4 (position 1) to 15.0% ± 0.7 (position 5) (means of 2 replicates measured twice).

Primary metabolites and adenine nucleotide quantification

The absolute and relative quantifications of primary metabolites in melon fruit were performed with ¹H NMR and GC–MS, respectively, as described by Biais et al. (2009). For ¹H NMR, fresh flesh pieces were squeezed and the juice was immediately flash frozen in liquid nitrogen. To stop enzymatic activities, 70% methanol-*d*₄ (v/v) was added prior to ¹H NMR acquisitions. For GC–MS, frozen ground samples were extracted with chloroform/methanol/water (1:2.5:1), derivatized, and quantification was performed using an internal standard.

Adenosine triphosphate (ATP), adenosine diphosphate (ADP) and adenosine monophosphate (AMP) were measured in neutralized perchloric acid extracts of frozen ground samples using a luciferin–luciferase method (Napolitano and Shain, 2005) and a luminescence ATP detection kit (PerkinElmer™, Zaventem, Belgium). The extraction was performed twice for each position, to be used as technological replicates. After an ATP calibration curve, the results were expressed as pmol mg_{FW}⁻¹ and calculated as the means of the values measured with four aliquot volumes of each extract, except if the saturation of the detector was observed. The adenylate energy charge (AEC) was calculated as follows: AEC = ([ATP] + 0.5[ADP]) / ([ATP] + [ADP] + [AMP]).

Data obtained for metabolites, nucleotides, the ATP/ADP ratio and AEC were analyzed using one-way analysis of variance (ANOVA) and Tukey's grouping using SAS Software v8.01 (SAS Institute, 1990).

Results and discussion

Metabolite gradients in melon fruit

The ¹H NMR and GC–MS profiling allowed absolute and relative quantification, respectively, of the main metabolites in melon fruit, including sugars, organic acids and amino acids. Fig. 2 presents the ¹H NMR concentration changes of six major sugars

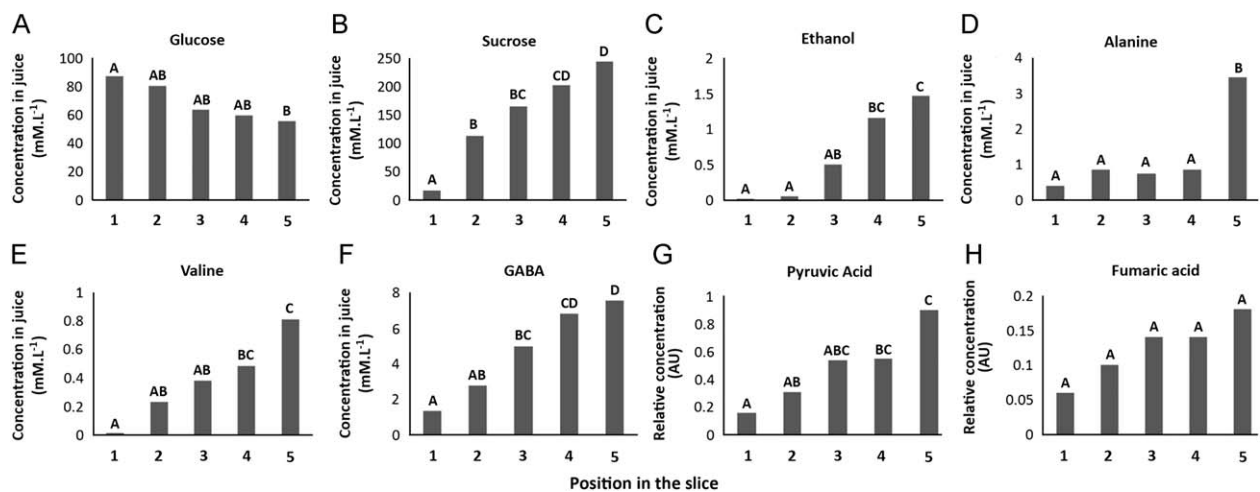


Fig. 2. Absolute concentration of some primary metabolites, determined using ¹H NMR profiling, depending on the location in the slice of melon fruit (Cézanne cv.). Concentrations are given in mM L⁻¹ of juice. (A) Glucose, (B) sucrose, (C) ethanol, (D) alanine, (E) valine and (F) GABA. Relative concentration of organic acids determined using GC–MS profiling, depending on the location in the slice of melon fruit. (G) Pyruvic acid and (H) fumaric acid. The results are the means of 4 measurements (2 samples × 2 technical replicates). Letters above histograms correspond to Tukey's groups. The values with the same letter are not statistically different (*P* < 0.05).

and amino-acids: glucose (A), sucrose (B), ethanol (C), alanine (D), valine (E) and GABA (F), and the GC–MS results obtained for two organic acids implicated in the glycolysis pathway, pyruvic acid (G) and fumaric acid (H). All these metabolites showed differences in concentration and distribution depending on the position in the slice. These results are in general agreement with the previous results (Biais et al., 2009). All metabolite concentrations, except for glucose, increased regularly from the skin (position 1) to the center of the fruit (position 5), indicating strong gradients. In the case of glucose (Fig. 2A), the gradient was inverted, i.e. the concentration decreased from the skin to the center of the fruit, suggesting a conversion of glucose to sucrose. This is in agreement with the concomitant decrease in the fructose content observed previously by mass spectroscopy (Biais et al., 2009). The fumaric acid gradient was not statistically significant. Nonetheless, its pattern showed a tendency to increase from the skin to the center of the fruit.

Adenine nucleotide gradients in melon fruit

In order to support the hypothesis further that *in situ* hypoxia activates fermentation processes and decreases the energy status, ATP, ADP and AMP were quantified (Fig. 3A). The total adenine nucleotide concentration was variable, but higher in the inner mesocarp (position 5) than in the epicarp (position 1). Position 1 contained a higher level of ATP (from 150 to 200 pmol mg⁻¹ FW) than ADP, which was very low in concentration (from 5 to 10 pmol mg⁻¹ FW) and AMP, which was almost undetected. In the mesocarp (positions 2–5), the ATP, ADP and AMP levels increased from the periphery (position 2) to the center of the fruit (position 5). Such an inverted bell-shaped spatial distribution of adenine nucleotides from the periphery to the center of the fruit is very

similar to what has been observed in potato tubers under normoxia (Geigenberger et al., 2000).

From these measurements, two parameters were calculated to probe for the changes in the energy status of melon. The ATP/ADP ratio showed a drastic decrease from 31.3 (position 1) to 5.7 (position 5) (Fig. 3B). The most important decrease in ATP/ADP ratio occurred between positions 1–2. The ATP/ADP ratio decreased from 31.3 to almost 8.2 between positions 1 and 2 and then reached a plateau at about 5–6 along the inner mesocarp (positions 3 and 5). The AEC dropped from 0.97 (position 1) to 0.83 (position 5) (Fig. 3B).

In situ hypoxia in melon flesh

Using melon juice for ¹H NMR metabolic profiling allowed for the quantification of volatile compounds such as ethanol (Fig. 2C). The ethanol concentration increased from the skin to the inner mesocarp. The presence of ethanol cannot be due to contamination or fermentation during the sampling, as juices were immediately deep frozen in liquid nitrogen and fixed with 70% deuterated methanol. This ethanol gradient may result from a fermentation process during fruit ripening. Two fermentation pathways exist in plants and are activated to regenerate NAD⁺ under low oxygen conditions. They first uses lactate dehydrogenase to produce lactate from pyruvate. It has been demonstrated that lactic acid production induces a cytosolic acidification (Roberts et al., 1989), which in turn rapidly activates the pyruvate decarboxylase (PDC). In the second fermentation pathway, PDC increases acetaldehyde, which is reduced to ethanol by alcohol dehydrogenase (Tadege et al., 1999). Fermentation being less efficient than respiration, the fermentation process induces an accumulation of pyruvate (Good and Muench, 1993), which in turn increases the amount of alanine synthesized by transamination reactions (Ismond et al., 2003). Moreover, low oxygen tension, by limiting the tricarboxylic acid (TCA) cycle activity, is known to induce an accumulation of organic acids in tomato roots (Gharbi et al., 2007). Our results showed a strong gradient of alanine and ethanol, indicating the activation of the fermentation pathways in the center of the fruit. Lactate was not detected, but is generally accumulated less in plant cells. Moreover, such an acidification could explain the parallel GABA gradient observed, as GABA is well known to be implicated in the pH regulation in cells (Crawford et al., 1994). Finally, the accumulation of pyruvic and fumaric acids (Fig. 3) in the center of the melon fruit strengthened the limitation of TCA cycle activity in this region. This is in agreement with the recent work of Pedreschi et al. (2009), who showed that increases in fumaric acid and GABA content were the main markers of hypoxia in pear fruit. The decrease in the ATP/ADP ratio (30 to 5–6) from the skin to the inner mesocarp is also in agreement with hypoxia and with the hypothesis of fermentation in melon fruit. Similar results were shown in potato tubers (Geigenberger et al., 2000), where the ATP/ADP ratio decreased from the periphery (9) to the center of the tuber (3). This could be explained by oxygen diffusion constraints within the fruit tissue, with the inner part of the fruit being less oxygenated, as described in pear fruits (Schotsmans et al., 2003). It is worth noting that hypoxia *in situ* in melon tissues was severe enough to change the ATP/ADP ratio, but not the adenylate energetic charge. This situation contrasts markedly with data obtained *in vitro* or *in vivo* in potato tubers, where O₂ delivery was artificially limited by low external O₂ partial pressure, leading to changes in AEC (Geigenberger et al., 2000).

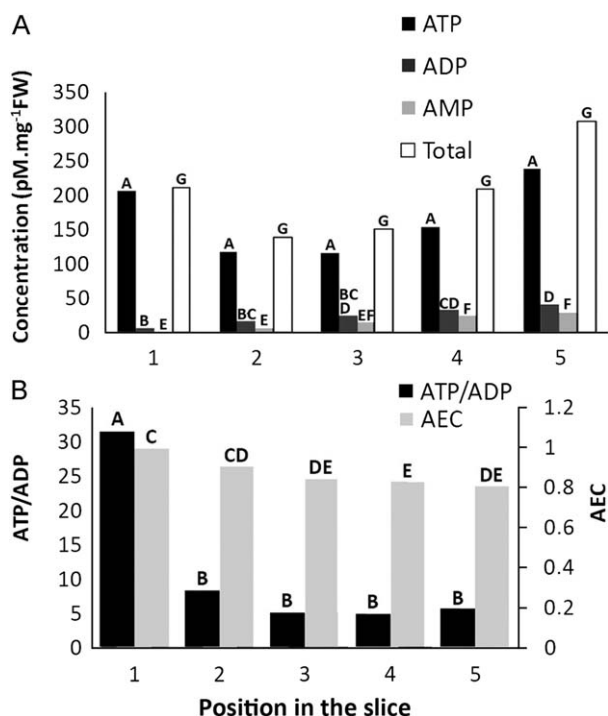


Fig. 3. (A) Concentration of ATP, ADP, AMP and total adenine nucleotides depending on the location in the slice of melon fruit (Cézanne cv.); (B) ATP/ADP ratio and adenylate energy charge (AEC). The results are the means of 4 measurements (2 samples × 2 technical replicates). Letters above histograms correspond to Tukey's groups. The values with the same letter are not statistically different ($P < 0.05$).

Conclusion

In this study, a metabolomics approach combining primary metabolites with adenine nucleotide quantification was used to

investigate the spatial localization of a number of metabolites and the energy status changes in melon fruit. Concentration gradients were shown for some sugars, amino-acids, organic acids and ethanol. The adenine nucleotide measurements in the fruit showed that, consistent with the alanine and ethanol gradient, the ATP/ADP ratio decreased drastically from the periphery to the center of the fruit. Taken together, these changes in metabolite concentrations reflect a decrease in the biosynthetic processes (accumulation of sucrose), an inhibition of the TCA cycle (accumulation of organic acids) and an activation of anaerobic metabolism (diversion of pyruvate to ethanol and alanine) by low oxygen tension. The remaining questions of how and when these gradients can take place during fruit development and ripening are under study. This will allow an understanding of how ethanol production occurs during the ripening step and how to limit this production, as ethanol can affect the organoleptic properties and consumer's acceptance. It may also highlight the new traits important for breeders to increase the Charentais melons' shelf-life.

Acknowledgments

This study was partially funded by the EU within the plant metabolomics project META-PHOR (FOOD-CT-2006-036220). We gratefully thank Sylvie Bochu and Françoise Leix-Henry from CEFEL (France) for providing the melon fruits, and Arthur

A. Schaffer (Volcani Center, Israel) and Dr. Robert Hall (Plant Research International, Holland) for critical reading of the manuscript.

References

- Biais B, Allwood JW, Deborde C, Xu Y, Maucourt M, Beauvoit B, et al. *Anal Chem* 2009;81:2884–94.
- Burger Y, Schaffer AA. *J Am Soc Hort Sci* 2007;132:704–12.
- Crawford LA, Bown AW, Breikreuz KE, Guinel FC. *Plant Physiol* 1994;104:865–71.
- de Melo MLS, Narain N, Bora PS. *Food Chem* 2000;68:411–4.
- Geigenberger P, Fernie AR, Gibon Y, Christ M, Stitt M. *Biol Chem* 2000;381:723–40.
- Gharbi I, Ricard B, Rolin D, Maucourt M, Andrieu M-H, Bizid E, et al. *Plant Cell Environ* 2007;30:508–17.
- Good AG, Muench DG. *Plant Physiol* 1993;101:1163–8.
- Ismond KP, Dolferus R, De Pauw M, Dennis ES, Good AG. *Plant Physiol* 2003;132:1292–302.
- Kourkoutas D, Elmore JS, Mottram DS. *Food Chem* 2006;97:95–102.
- Lalonde S, Tegeder M, Throne-Holst M, Frommer WB, Patrick JW. *Plant Cell Environ* 2003;26:37–56.
- Napolitano MJ, Shain DH. *J Biochem Biophys Methods* 2005;63:69–77.
- Pedreschi R, Franck C, Lammertyn J, Erban A, Kopka J, Hertog M, et al. *Postharvest Biol Technol* 2009;51:123–30.
- Roberts JKM, Chany K, Webster C, Collis J, Walbot V. *Plant Physiol* 1989;89:1275–8.
- SAS Institute. *SAS/STAT User's Guide*, v6, 4th ed. SAS Institute Inc. 1990.
- Schotsmans W, Verlinden BE, Lammertyn J, Nicolai BM. *Postharvest Biol Technol* 2003;29:155–66.
- Stepansky A, Kovalski I, Schaffer AA, Perl-Treves R. *Genet Resour Crop Evol* 1999b;46:53–62.
- Sugiyama J. *J Agric Food Chem* 1999;47:2715–8.
- Tadege M, Dupuis I, Kuhlemeier C. *Trends Plant Sci* 1999;4:320–5.